

Nonideal equation of state in the pseudo-potential lattice Boltzmann methods

Sigvat K. Stensholt

Centre for Integrated Petroleum Research (Uni CIPR), Bergen, Norway

Alf H. Øien and Inga Berre

Department of Mathematics, University of Bergen, Bergen, Norway

(Dated: April 13, 2010)

Abstract

A nonideal equation of state using nearest-neighbor interactions is investigated for the multi-component multiphase Shan-Chen model. We find that by defining the equation of state through nearest-neighbor interactions, a more accurate pressure field can be obtained, and we achieve good adherence to Laplace's law even for low values of the separation parameter and small droplets. A more accurate pressure field allows more accurate estimates of the surface tension coefficient.

INTRODUCTION

Since the lattice Boltzmann method was introduced in 1988 by McNamara and Zanetti [1], it has become a popular alternative to traditional Navier-Stokes solvers for fluid flow. The model simulates flow by tracking the discrete distribution function. The rules for interparticle collisions and particle movement are simple, and its structure makes parallel processing very feasible [2].

Only a few years after the method was introduced, different schemes to extend the method to multiphase flow were proposed. In chronological order, these include the color model [3], the pseudo-potential models [4, 5], and the free energy models [6, 7]. In this article, we use the pseudo-potential model, also called the “Shan-Chen” method, to investigate multicomponent multiphase (MCMP) flow. This model features two components that exert a repulsive force on each other, driving them apart and forming two distinct phases.

In single-phase flow, pressure variations are due to slight variations in density, and an ideal equation of state is used. However, the forces in the Shan-Chen model add nonideal terms to the equation of state which are especially significant near the interfaces. For the Shan-Chen model, equations of state have been studied extensively for the single-component case [8, 9].

A common test to verify that a lattice-Boltzmann model for multiphase flow is reasonable, is to check that Laplace’s law holds for static, circular droplets. The pressure difference between the interior and exterior of a droplet should be proportional to the reciprocal of the droplet’s radius. A numerical example by Shan and Chen [4] showed that their model respected Laplace’s law when the pressure p was calculated using the ideal gas equation.

Our observation is that this adherence to Laplace’s law relies on a moderately large separation parameter and reasonably large droplets. When simulating fluids with a very low surface tension, diffusive effects cause anomalous results, especially for small droplets. However, the issue may be remedied by including nonideal terms in the pressure. In this article, we improve on the traditional nonideal equation of state and show that the best results are achieved if nearest-neighbor terms are accounted for. This improved equation of state allows more accurate estimates of the surface tension coefficient.

LATTICE BOLTZMANN METHOD

The purpose of the Lattice Boltzmann method is to track a particle distribution function $f_i(\mathbf{x}, t)$ on a discrete lattice. In a multicomponent model, each component has its own distribution function. Particles may move to neighboring nodes along velocity vectors \mathbf{e}_i . On a regular two-dimensional square lattice with diagonal movement and rest particles (also called a D2Q9 lattice [10]), \mathbf{e}_i is given by

$$\mathbf{e}_i = \begin{cases} (0, 0) & i = 0, \\ (\sin(i\pi/2), -\cos(i\pi/2)) & i = 1, 2, 3, 4, \\ \sqrt{2}(\cos(\frac{i-5\pi}{2} + \frac{\pi}{4}), \sin(\frac{i-5\pi}{2} + \frac{\pi}{4})) & i = 5, 6, 7, 8. \end{cases} \quad (1)$$

From the distribution function, the mass density ρ and momentum $\rho\mathbf{u}$ can be calculated as

$$\rho(\mathbf{x}, t) = m \sum_i f_i(\mathbf{x}, t), \quad (2)$$

$$\rho(\mathbf{x}, t)\mathbf{u}(\mathbf{x}, t) = m \sum_i f_i(\mathbf{x}, t)\mathbf{e}_i, \quad (3)$$

where m is the particle mass.

The distribution function f_i is updated at each time step through the equation

$$f_i(\mathbf{x} + \mathbf{e}_i, t + 1) = f_i(\mathbf{x}, t) + \Omega_i, \quad (4)$$

where the first terms represent advection while the Ω_i term accounts for interparticle collisions. For simplicity, we use the single-relaxation time model based on the Bhatnagar, Gross, Krook (BGK) operator [11]. The BGK operator features a relaxation to an equilibrium distribution function f_i^{eq} and is given by

$$\Omega_i = \frac{1}{\tau}(f_i - f_i^{eq}) \quad (5)$$

$$f_i^{eq} = w_i \frac{\rho}{m} \left(1 + \frac{3(\mathbf{e}_i \cdot \mathbf{u})}{c_s^2} + \frac{9(\mathbf{e}_i \cdot \mathbf{u})^2}{2c_s^4} - \frac{3\mathbf{u}^2}{2c_s^2} \right), \quad (6)$$

where $c_s = \frac{1}{\sqrt{3}}$ is the speed of sound, the weights w_i are given by

$$w_0 = \frac{4}{9}, \quad w_{1,2,3,4} = \frac{1}{9}, \quad w_{5,6,7,8} = \frac{1}{36}, \quad (7)$$

and the relaxation time parameter τ is related to the kinematic viscosity ν through the relation

$$\nu = \frac{2\tau - 1}{6}. \quad (8)$$

The terms for the equilibrium distribution (6) can be derived from Gauss-Hermite quadrature. Validity of the BGK operator is dependent on a low Mach number [12].

Pressure variations in lattice Boltzmann methods arise from small variations in density. When there are no large internal separation forces, the pressure can be calculated using the ideal gas equation

$$p = c_s^2 \rho. \quad (9)$$

Shan-Chen model

Both the single-component and multicomponent Shan-Chen models for multiphase flow were introduced in 1993 [4]. The multicomponent version was studied deeper by Shan and Doolen [13].

In the multicomponent model, we need two distribution functions, f_i^R and f_i^B , where R and B stand for the “red” and “blue” components. These generic terms are placeholders for real fluids, for example, “red” may represent oil while “blue” represents water. We let the superscript a stand for an arbitrary component, whereas \hat{a} represents the other component. Each of these distributions evolve as in equation (4). A common velocity \mathbf{u}' for all fluids at the site is calculated by [14]

$$\mathbf{u}' = \frac{\sum_{a=R,B} \sum_i \frac{f_i^a \mathbf{e}_i}{\tau^a}}{\sum_{a=R,B} \frac{\rho^a}{\tau^a}}. \quad (10)$$

The interaction between the fluids in the Shan-Chen model stems from repelling forces between red and blue particles. In particular, the force \mathbf{F}^a on phase a caused by the presence of phase \hat{a} is given by

$$\mathbf{F}^a = -\rho^a(\mathbf{x}, t) G^{a\hat{a}} \sum_{i=1}^8 w_i \rho^{\hat{a}}(\mathbf{x} + \mathbf{e}_i) \mathbf{e}_i. \quad (11)$$

The parameter $G^{a\hat{a}}$ controls the strength of the separation, and controls several aspects such as surface tension, phase purity, and interface thickness. From the force in equation (11), each of the components receive an individual velocity \mathbf{u}^a calculated by [14]

$$\mathbf{u}^a = \mathbf{u}' + \frac{\tau^a \mathbf{F}^a}{\rho^a}. \quad (12)$$

Maintaining symmetry in the forces requires $G^{a\hat{a}} = G^{\hat{a}a}$. In order to obtain phase separation, the separation forces in equation (11) must be strong enough to overcome the diffusive effects. This happens for a critical $G_C^{a\hat{a}}$, if $G^{a\hat{a}}$ is below this value the phases will simply dissolve

into one another leaving a uniform mixture. The value of $G_C^{a\hat{a}}$ is dependent on a number of factors, including the relaxation parameters τ^R and τ^B , and the densities ρ^R and ρ^B . If $\rho^R + \rho^B$ is fixed, G_C^{RB} is smallest if $\rho^R = \rho^B$ and increases as the density ratio between the most and least abundant component increases [15]. Generally, the surface tension increases with larger G^{RB} and smaller τ^R and τ^B [16]. Sharper and less diffusive interfaces can be obtained by increasing $G^{a\hat{a}}$. However, large forces create large velocities which violate the assumption of a low Mach number and may destabilize the numerical stability of the model. This limits the magnitude of $G^{a\hat{a}}$ [17]. The choice of separation parameter is also limited by the surface tension we wish to simulate, if we want to simulate flows where the surface tension is small, we need to employ a small $G^{a\hat{a}}$ and accept more diffusive interfaces.

Evaluation of pressure

The anomalous pressure readings for low G are a consequence of the impurity of the phases. When there is a significant number of blue particles dissolved in the droplet (red phase), the separation forces are non-trivial and the density becomes lower than it would be if the phases were pure. Shan and Chen observed that the ideal gas equation could be used in a single component region [4], but for low G^{RB} close to G_C^{RB} , these regions are not single component. Therefore, nonideal pressure terms are needed to obtain proper estimates for pressure.

Shan and Doolen [13] give an equation of state that accounts for the mixing. This has been used extensively, including articles by Kang et al.[18] and Huang et al.[14]. The equation of state is given by

$$p(\mathbf{x}) = \sum_a \rho^a(\mathbf{x})c_s^2 + \frac{1}{3}G^{RB}\rho^R(\mathbf{x})\rho^B(\mathbf{x}). \quad (13)$$

This equation adds nonideal terms to the pressure compensating for the lower interface density. However, all the terms in equation (13) depend on the local densities in \mathbf{x} only, and not the nearest neighbors.

Calculating the nonideal pressure using only the local particle densities creates a dependence on the interface's alignment with the underlying lattice. For example, if a perfectly sharp interface runs between two fluid sites, so that the neighboring fluid sites on either side of the interface are purely red or blue, the nonideal pressure term will be zero. However, if the interface passes through a fluid node so that the interfacial site contains a mixture of red

and blue particles, the nonideal term will be non-zero. While the Shan-Chen model does not produce perfectly sharp interfaces, the issue remains that nonideal pressure arises from the interaction of opposite components in neighboring sites, something which is not accounted for in equation (13). We have therefore used another expression for nonideal equation of state which involves the nearest-neighbors. This is inspired by the fact that the full pressure tensors, found in Shan and Chen’s 1994 paper [5] and He and Doolen [19], involve gradients and thus also accounts for nearest-neighbor interactions.

We propose the following equation of state:

$$p(\mathbf{x}) = \sum_a \rho^a(\mathbf{x}) c_s^2 + \frac{3}{10} \sum_{a=R,B} \rho^a(\mathbf{x}) G^{aa} \sum_{i=1}^8 w_i \rho^{\hat{a}}(\mathbf{x} + \mathbf{e}_i). \quad (14)$$

Note that if $\rho^a(\mathbf{x})$ and $\rho^{\hat{a}}(\mathbf{x})$ are constant in \mathbf{x} , equation (14) is equivalent to equation (13).

NUMERICAL EXPERIMENTS

Laplace’s law

When there are two immiscible fluids, a typical phase pattern consists of a *disperse phase* which forms circular droplets inside a *continuous phase*. The pressure inside the droplets is higher than the pressure outside, and at steady state, the pressure difference is given by Laplace’s law

$$\Delta p = \frac{\sigma}{r}, \quad (15)$$

where r is the droplet’s radius and σ is the surface tension coefficient.

Laplace’s law (15) is a fundamental result in multiphase flow, and all two-phase lattice Boltzmann methods have been tested to verify that simulated droplets adhere to Laplace’s law.

Laplace’s law has a very specific application in Shan-Chen simulations. As mentioned in , σ increases with G^{RB} and decreases with τ , but as the Shan-Chen is not based on thermodynamic principles, the relationship between σ , τ^R , τ^B , and G^{RB} can only be found experimentally [16]. The simplest way is using $r\Delta p$ as an estimate for σ , when there are several drops a least-square approximation can be used. Obviously, an incorrect figure for Δp will disturb the correct determination of σ .

Shan and Chen's original article [4] generated a set of random droplets from an initially uniform mixture and plotted the particle density difference between the droplets' interiors against the inverse of the droplets' radii. For their choice of parameters, their plot affirmed the linear relationship which Laplace's law (15) predicts.

Simulations and results

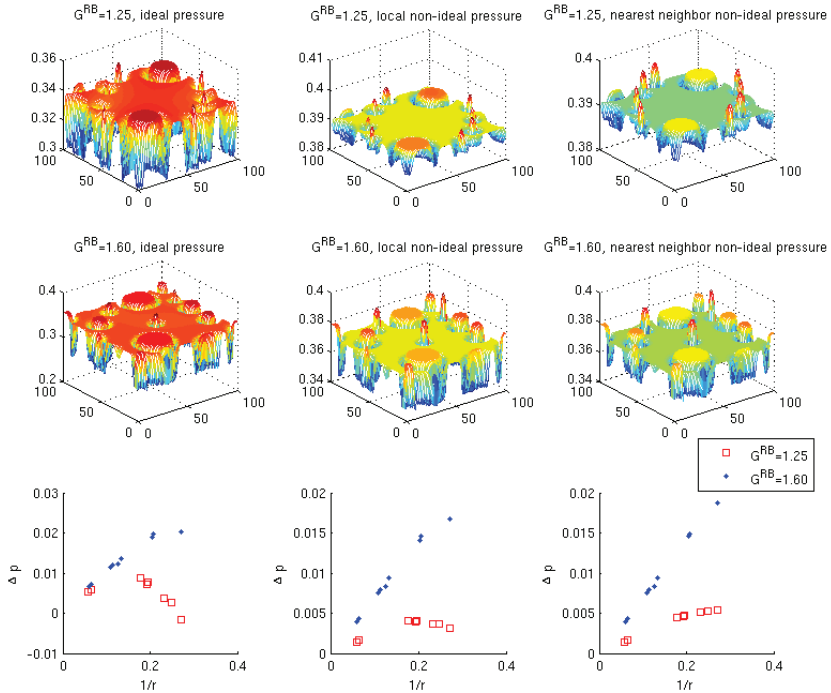


FIG. 1. (Color online) Pressure fields with $G^{RB} = 1.25$ (top row) and $G^{RB} = 1.6$ (second row), and pressure difference $p^R - p^B$ between the interior and exterior versus the inverse of the radius of the droplets (third row). In the left column, pressure is measured using the ideal gas equation (9). In the middle column, the pressure is measured using the nonideal gas equation (13) with local terms only. In the figures in the right column, pressure is measured using the nonideal gas equation (14) with contributions from the nearest neighbors. The average density is 1, and $\tau^R = \tau^B = 1$.

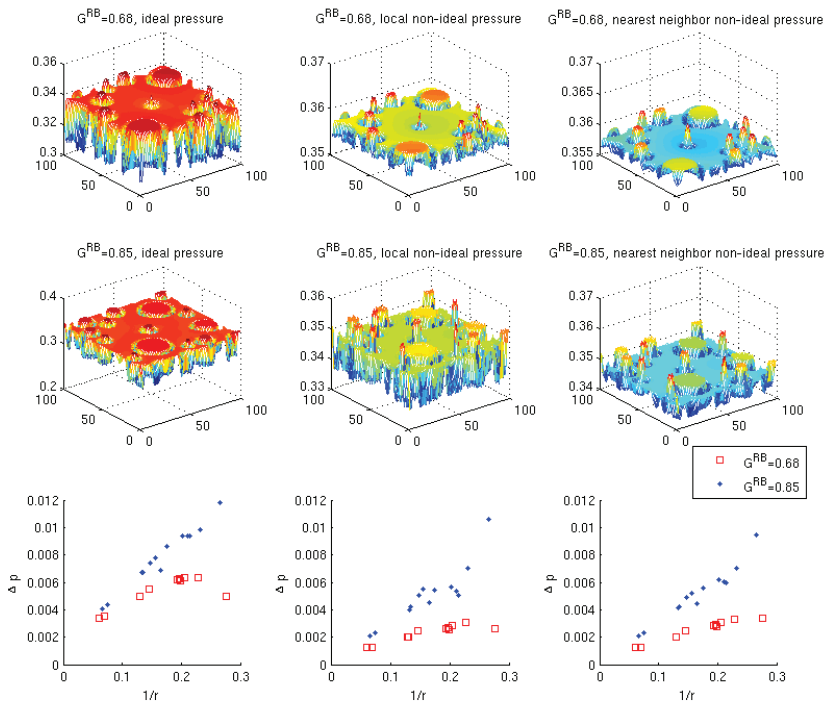


FIG. 2. (Color online) Pressure field and pressure difference $p^R - p^B$ between the interior and exterior versus the inverse of the radius of the droplets. The columns from left to right represent pressures calculated from equations (9), (13), and (14). Relaxation parameters $\tau^R = \tau^B = \frac{2}{3}$.

We have run two sets of experiments, with different values of the separation parameters τ^R and τ^B , for the purpose of generating a set of droplets with different radii. In both cases, the simulations are conducted on a 100×100 grid with periodic boundary conditions. The particle mass for both components is 1 and the average total density $\rho^R + \rho^B = 1$. 30% of the particles are red, while the remaining 70% are blue. A slight difference from Shan and Chen's experiment is that we seeded some droplets at $t = 0$ in order to ensure a wide range of droplet radii. Pressure measurements according to equations (9), (13), and (14) were taken at $t = 10000$. Another difference is that we conducted experiments on a square grid, while Shan and Chen used a triangular grid.

In the first case, we set $\tau^R = \tau^B = 1.0$. In this case, we found $G_C^{RB} \approx 1.22$, and we conducted simulations with $G^{RB} = 1.25$ and $G^{RB} = 1.60$. The pressure fields, interpreted according to equations (9), (13), and (14) for this set of experiments are shown in Figure 1. We have also plotted the pressure difference Δp against the reciprocal of each droplet's radius.

In the second case, we have $\tau^R = \tau^B = \frac{2}{3}$. In this case, we found that $G_C^{RB} \approx 0.66$, and we conducted simulations with $G^{RB} = 0.68$ and $G^{RB} = 0.85$. The pressure fields and Δp versus $\frac{1}{r}$ plots for this set of experiments are shown in Figure (2).

DISCUSSION

Our simulations on static droplets using the Shan-Chen model show that the observation of Laplace's law using the ideal gas equation only occurs when G^{RB} is moderately large, and the radius of the droplets are much larger than the interface width. If these conditions are not met, the ideal pressure will not respect Laplace's law.

In our first simulation, with $\tau^R = \tau^B = 1.0$ and $G = 1.60$, we find that Δp is indeed proportional to r^{-1} for droplets with a radius of about 5 or larger as seen in Figure 1. However, the data point for the smallest droplet does not align well with the data points for the larger droplets. With $G^{RB} = 1.25$, slightly over G_C^{RB} , the interfaces are wider and more diffuse, and the ideal pressure's adherence to Laplace's law breaks down for larger droplets than was the case with $G^{RB} = 1.60$. We observe that the pressure inside the smallest droplet is lower than in the continuous phase. The smallest droplet has a radius of about 3 cells, and even its center is in effect part of the interface, giving this droplet a very low density. This effect which breaks Laplace's law for low G^{RB} and small droplets when p is calculated from the ideal gas equation.

The pressure field using the nonideal gas equation based on local densities (13) gives an improvement, and we see that the pressure difference Δp is positive for all the droplets. However, plotting the pressure against the inverse of the radius shows that the smallest droplets still deviate from the straight line predicted by Laplace's law. With $G^{RB} = 1.25$, the pressure difference decreases with $\frac{1}{r}$ for $r < 5$.

The pressure field using the nonideal gas equation based on nearest-neighbor densities (14) provides the best result. With $G^{RB} = 1.0$ and $\tau^R = \tau^B = 1.0$, the data point for the

smallest droplet aligns well with the other data points. With $G^{RB} = 1.25$, only (14) shows Δp consistently increasing with $\frac{1}{r}$.

With $\tau^R = \tau^B = \frac{2}{3}$, and $G^{RB} = 0.68$, we again see that equations (9) and (13) yield pressures which deviate significantly from Laplace's law for the smallest droplets. Although the pressure calculated from (14) does not correspond exactly to Laplace's law, the relationship between Δp and r^{-1} comes closer to a straight line than the other equations for pressure. With the larger $G^{RB} = 0.85$, Laplace's law is again approximately observed using the ideal gas equation. With equation (13) we see a clear positive correlation between $\frac{1}{r}$ and Δp , although the data points deviate significantly from a straight line. The data points using equation (14) for pressure deviate less from Laplace's law.

CONCLUSIONS

The Shan-Chen model is a diffuse interface model, so it is essential to employ a nonideal equation of state obtain an accurate pressure field. The common nonideal equation of state (13) does not account for nearest neighbor interactions, and while it is an improvement over the ideal gas equation, it can break down for small droplets. By taking into account the nearest-neighbor interactions in the equation of state, the accuracy of the pressure field is considerably enhanced, and Laplace's law is acknowledged even when the interfaces are highly diffusive. The improved adherence to Laplace's law obtained from equation (14) allows us to obtain better estimates for the surface tension coefficient.

For moderate G^{RB} , the ideal gas equation will yield adherence to Laplace's law, albeit with a different estimate for the surface coefficient σ . Including nonideal terms should give a more accurate estimate of the surface tension coefficient. The benefit of using equation (14) instead of equation (13) is greatest when the droplets are small and when G^{RB} is only slightly larger than the critical G_C^{RB} .

[1] G. R. McNamara and G. Zanetti, Phys. Rev. Lett., **61**, 2332 (1988).

[2] S. Succi, *The Lattice Boltzmann Equation for Fluid Mechanics and Beyond* (Oxford Science Publications, 2001).

- [3] A. K. Gunstensen, D. H. Rothmann, S. Zaleski, and G. Zanetti, *Phys. Rev. A*, **43**, 4320 (1991).
- [4] X. Shan and H. Chen, *Phys. Rev. E*, **47**, 1815 (1993).
- [5] X. Shan and H. Chen, *Phys. Rev. E*, **49**, 2941 (1994).
- [6] E. Orlandini, M. R. Swift, and J. M. Yeomans, *Europhys. Lett.*, **32**, 463 (1995).
- [7] M. R. Swift, W. Osborn, and J. Yeomans, *Phys. Rev. Lett.*, **75**, 830 (1995).
- [8] A. Kupershtokh, D. Medvedev, and D. Karpov, *Comput. Math. Appl.*, **58**, 965 (2009).
- [9] P. Yuan and L. Schaeffer, *Phys. Fluids*, **18**, 042101 (2006).
- [10] Y. H. Qian, D. D’Humières, and P. Lallemand, *Europhys. Lett.*, **17**, 479 (1992).
- [11] P. L. Bhatnagar, E. P. Gross, and M. Krook, *Phys. Rev.*, **94**, 511 (1954).
- [12] X. He and L.-S. Luo, *Phys. Rev. E*, **56**, 6811 (1997).
- [13] X. Shan and G. Doolen, *J. Stat. Phys.*, **81**, 379 (1995).
- [14] H. Huang, D. T. Thorne, M. G. Schaap, and M. C. Sukop, *Phys. Rev. E*, **76** (2007), 066701.
- [15] N. S. Martys and J. F. Douglas, *Phys. Rev. E*, **63**, 031205 (2001).
- [16] J. Chin, E. S. Boek, and P. V. Coveney, *Phil. Trans. R. Soc. A*, **360**, 547 (2002).
- [17] M. C. Sukop and D. T. Thorne, *Lattice Boltzmann Modeling, An Introduction for Geoscientists and Engineers* (Springer, 2006).
- [18] Q. Kang, D. Zhang, and S. Chen, *Phys. Fluids*, **14**, 3203 (2002).
- [19] X. He and G. D. Doolen, *J. Stat. Phys.*, **107**, 309 (2002).